An optical fiber-based source of polarization-entangled photon pairs

Jingyun Fan*, Matthew D. Eisaman, and Alan Migdall

Optical Technology Division, National Institute of Standards and Technology
100 Bureau Drive, Mail Stop 8441, Gaithersburg. MD 20899-8441
and
Joint Quantum Institute, University of Maryland, MD 20742

ABSTRACT

We describe the preparation of a high spectral brightness, broad wavelength coverage, single-spatial mode source of polarization-entangled photon pairs operated at room temperature. The source takes advantage of single-mode fiber optics, highly nonlinear microstructure fiber, judicious phase-matching, and the inherent stability provided by a Sagnac interferometer. With a modest average pump power (300 μW), we create all four Bell states with a detected two-photon coincidence rate of 7 kHz per bandwidth of 0.9 nm, in a spectral range of more than 20 nm.

Keywords: four-wave mixing, Sagnac interferometer, quantum tomography

1. INTRODUCTION

In recent years, fundamental and practical questions regarding quantum entanglement have led to fruitful research, ranging from tests of fundamental quantum-mechanical principles, to quantum-information applications such as quantum non-locality,[1] quantum-key distribution,[2] and quantum-state teleportation.[3,4] For example, it is now well-known that two parties, each sharing half of an entangled photon pair, can use this entanglement to communicate with absolute security.[5] Despite the rapid progress over the last decade toward the practical application of these ideas, many challenges remain. In particular, for real-world quantum communication and cryptography applications to take advantage of entanglement, we need a robust source of entangled photon pairs with high spectral brightness, broad wavelength coverage, and a single-mode spatial output that is compatible with fiber networks or free-space operation.

Since the demonstration of two-photon light created by spontaneous parametric down conversion (SPDC) in a nonlinear crystal by Weinberg in 1970,[6] thirty years of optimization have led to bright two-photon sources.[7-9] In SPDC, a pump photon at a high frequency ω_P is converted into two lower energy photons, satisfying energy conservation $\omega_P = \omega_s + \omega_i$, and the phase-matching condition, $\vec{k}_P = \vec{k}_s + \vec{k}_i$. In a nonlinear crystal, pairs of photons are often emitted into a large number of spatial and spectral modes. However, for communication applications, light must be delivered in single spatial mode and preferably with a narrow spectral bandwidth. A large collection loss is often inevitably encountered when one uses a SPDC as the source.

An ideal source of two-photon entanglement for quantum information applications should have high two-photon spectral brightness, a broad spectral range, output in a single-spatial mode, negligible noise background, efficient collection and delivery, and compact physical size. Those who are familiar with fiber optics will immediately think of high gain fiber parametric amplifiers. Such amplifiers have been

* jfan@nist.gov

Quantum Communications Realized
edited by Yasuhiko Arakawa, Masahide Sasaki, Hideyuki Sotobayashi,
Proc. of SPIE Vol. 6780, 67800Q, (2007) · 0277-786X/07/$18 · doi: 10.1117/12.734591

extensively studied at high powers for optical signal amplification for communication networks. Its low power extreme may be ideal for two-photon generation. Here, a parametric four-photon process, where two pump photons are consumed to produce two output photons, occurs. We now detail the fundamental issues and the figures of merit in making an all fiber-based source of polarization-entangled photon pairs.

2. NONLINEAR FIBER OPTICS

A typical single-mode optical fiber (SMF) is made of fused silica and is cylindrically symmetric. With proper core size and refractive index difference between fiber core and the cladding, light propagates in a single-spatial mode with low loss. The small effective mode area (A_{eff}) of the light beam inside the SMF, (about 50 μm^2 for λ = 1.55 μm), together with a long fiber length (L), leads to a high overall nonlinear interaction that is proportional to PL/A_{eff}, where P is the input power. Because glass is centrosymmetric, second order nonlinear susceptibility, $\chi^{(2)}$, is absent in the SMF. Hence the prominent nonlinear interactions in a SMF are $\chi^{(3)}$ processes. Among the third order nonlinear processes, the most important ones for the creation of two-photon light are spontaneous four-wave mixing (SFWM) and spontaneous Raman scattering (RS). SFWM and RS typically occur together.

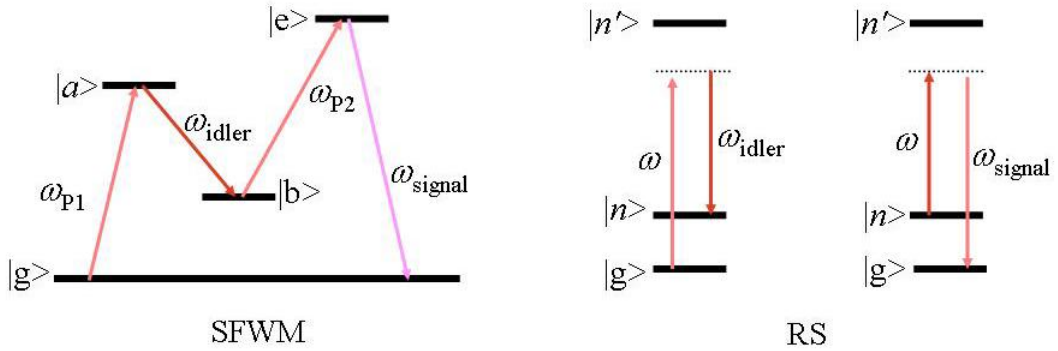

Fig.1. Energy diagrams for spontaneous four-wave mixing (SFWM) and Raman scattering (RS). In SFWM, two photons are absorbed from the pump fields (ω_{P1} and ω_{P2}) to create two new photons ω_{signal} and ω_{idler} that are correlated due to energy conservation. In Raman, a single pump photon interacts with a phonon to produce a photon of higher/lower energy $\omega_{\text{signal}}/\omega_{\text{idler}}$.

From Fig. 1, we readily see the physical origin of twin photon generation. Here, two pump photons (ω_{P1} and ω_{P2}) are consumed to create two new photons ω_{signal} and ω_{idler}. The two new photons ω_{signal} and ω_{idler} are created simultaneously to satisfy energy conservation. Because the two modes: signal and idler, have initially no photons in them, the newly created twin photons are perfectly correlated. For cryptography, the signal photon can be sent out as the carrier, while the idler is detected as a trigger or a mark that a signal photon is generated and sent out. The main source of error that can destroy this perfect correlation is the Raman process. For example, if the Raman process only adds a signal photon without the idler, it will spoil the correlation and the certainty.

The efficiency and spectrum of SFWM is mainly governed by phase-matching which is determined by fiber dispersion and Kerr-nonlinearity (n_2).[10] The fiber dispersion contains both material dispersion and waveguide dispersion. It constitutes the propagation phase-mismatch $\Delta kz = (k_{P1} + k_{P2} - k_{signal} - k_{idler})z$ of the four different optical fields in the SMF. The Kerr-nonlinearity is the optical power-induced variation of refractive index that causes a phase-modulation of the co-propagating electric fields by $\gamma(P_1 + P_2)z$. Here, γ is the nonlinear gain coefficient with $\gamma = \dfrac{2\pi n_2}{\lambda A_{eff}}$.

When these two phases cancel in a SMF, the SWFM is phase-matched, with $\Delta kz + \gamma(P_1 + P_2)z = 0$.

Energy is transferred from the pump fields (ω_{P1} and ω_{P2}) to the initially absent signal (ω_{signal}) and idler (ω_{idler}) fields as the four fields propagate together in the fiber.

The Raman process in a fused silica SMF has been long known. Fundamentally, pump photons induce transitions in the fiber glass vibrational bands. This is frequently described as an inelastic scattering process and characterized as a phonon exchange process. The amorphous nature of fused silica spreads the otherwise limited Raman transition bandwidth into a continuum. The RS spectrum in a fused silica SMF extends for about 40 THz ($\Delta\omega$, detuning from the pump frequency) and peaks at $\Delta\omega \approx 13$ THz. In addition, the RS process can cascade if pump power is high enough to drive secondary RS processes. At low power, the first order RS spectrum represents the single-photon noise distribution, which must be accounted for in the creation of a fiber-based two-photon light source.

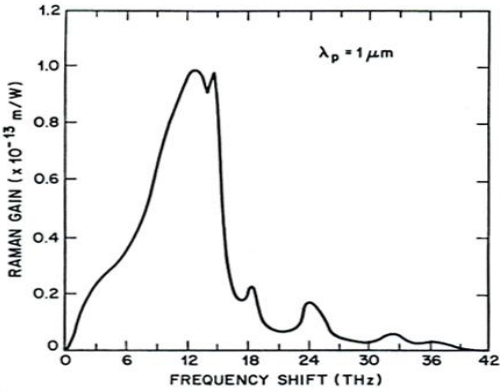

Fig.2 Raman scattering gain in a typical fused silica SMF.

We noticed two important technical facts that became useful in the preparation of a fiber-based source of two-photon light. First, the gain of phase-matched SFWM at low power is proportional to $(\gamma PL)^2$ $\propto (n_2 \cdot \frac{1}{A_{eff}} \cdot PL)^2$. While one can increase the SFWM gain by increasing the product of PL, this also adds unwanted multi-photon emission through stimulated FWM and RS processes. This can be avoided by reducing the effective fiber area, using microstructure fibers (MF). Another advantage is to aid the phase-matching conditions, using the MF's controllable dispersive behavior.

An MF is a one-dimensional photonic crystal patterned with periodic air-holes running parallel to the fiber's optical axis, with one of the air holes missing. The region with the missing hole serves as the fiber core with the surrounding air hole region acting as a cladding with a lower refractive index. Because the air-hole region can be engineered to be mostly holes with very little glass, the cladding index can approach one. The large refractive index difference between the core and the cladding allows us to make the core size very small while allowing a very broad spectral range of wavelengths to propagate in a single spatial mode with low loss, thus creating what is referred to as (spectrally) endless single-mode fiber.[11] The effective mode area of a MF is typically one order of magnitude smaller than that of the conventional SMF, increasing the effective fiber nonlinearity by 10x. Because of this higher nonlinearity, lower pump powers are applied to achieve the same two-photon signal. Because the Raman background is simply linearly proportional to the pump power, it is possible to significantly improve the two-photon coincidence/two-photon accidental coincidence (C/A) ratio with an MF.

Making the fiber core smaller not only effectively increases the fiber nonlinearity, it also moves λ_{ZDW} to shorter wavelengths. This provides additional flexibility in designing fiber with appropriate dispersion properties to create two-photon light by SFWM at a range of desired wavelengths to meet different applications.

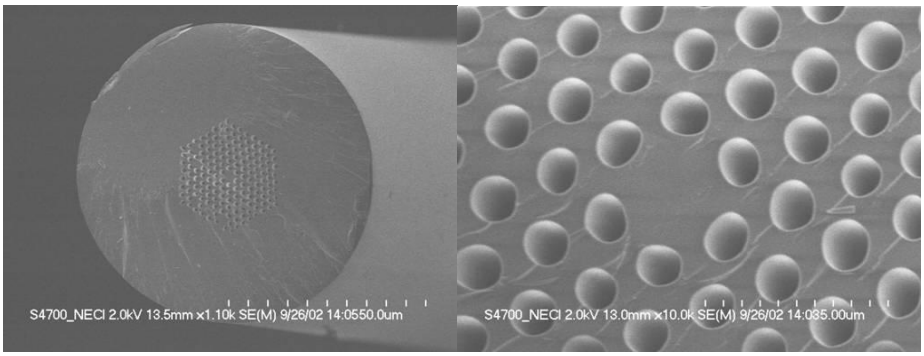

Fig.3 Scanning Electron Microscopy (SEM) image of a microstructure fiber

3. A BRIGHT ROBUST SOURCE OF POLARIZATION-ENTANGLED PHOTON PAIRS

In previous three-wave (down-conversion) or four-wave mixing schemes producing entangled photon pairs, two photon pairs (H_sH_i and V_sV_i, H: horizontal polarization, V: vertical polarization) were created separately, and then interferometrically combined to be indistinguishable. The need for the two photon pairs to be indistinguishable requires precise mode control and stability. Achieving this in a three-wave process is possible, but at the cost of flexibility in spectral mode selection.[7-9] Four-wave schemes offer less stability because of temporal coherence drifts between the two pump beams required, but more flexibility in spectral-mode selection.[12,13] To achieve both source stability and easy spectral selectivity, we introduce a new design that uses a polarization-configured single-mode optical-fiber Sagnac interferometer.

The experimental setup is shown in Fig. 4. After passing through a transmission grating, the 8 ps pump laser pulse (λ_P = 740.7 nm, repetition rate of 80 MHz) is incident onto a polarizing beam splitter (PBS), splitting into a horizontally (H)-polarized pump pulse (exiting port B of PBS) and a vertically (V)-polarized pump pulse (exiting port A of PBS). An 1.8-meter polarization-maintaining microstructure fiber (PMMF, zero-dispersion wavelength λ_{zdw} = 745 +/- 5 nm, nonlinearity γ = 70 $W^{-1}km^{-1}$ at λ_P) is arranged with its principal axis oriented horizontally at one end to accept (or output) the H-polarized light beam from (or to) port B and oriented vertically at the other end to accept (or output) the V-polarized light beam from (or to) port A. The PMMF and the PBS form a polarization-configured fiber Sagnac interferometer. With the small spatial-mode size of the microstructure fiber made possible by the large index difference between the glass core and air cladding, and the resulting high optical intensities, the PMMF exhibits high SFWM gain at large detuning from the pump wavelength where the Raman gain is lower. The PMMF has the additional property that it maintains a single spatial mode for all wavelengths coupled in along its principal axis, as well as maintaining a single polarization mode. The polarization extinction ratio of the fiber Sagnac interferometer is measured to be better than 300:1.

The two pump pulses counter-propagate along the same principal axis in the PMMF. The bi-photon states produced through SFWM by the H-polarized pump pulse, which is coupled into the PMMF through port B of the PBS, are output via port A in the V-polarization state ($V_s(\omega)V_i(-\omega)$, ω is the frequency detuning from the pump wavelength, $\omega = \omega_s - \omega_P = \omega_P - \omega_i$). The bi-photon states produced by the V-polarized pump pulse, which is coupled into the PMMF through port A of the PBS, are output via port B in the H-polarization state ($H_s(\omega)H_i(-\omega)$). These two SFWM processes, driven by equal-power, counter-propagating laser pulses, produce equal outputs. Upon exiting, the cross-polarized bi-photon states coherently overlap at the PBS to produce polarization-entangled Bell states in the form of $\Phi^+(\omega) = H_s(\omega)H_i(-\omega) + V_s(\omega)V_i(-\omega)$.

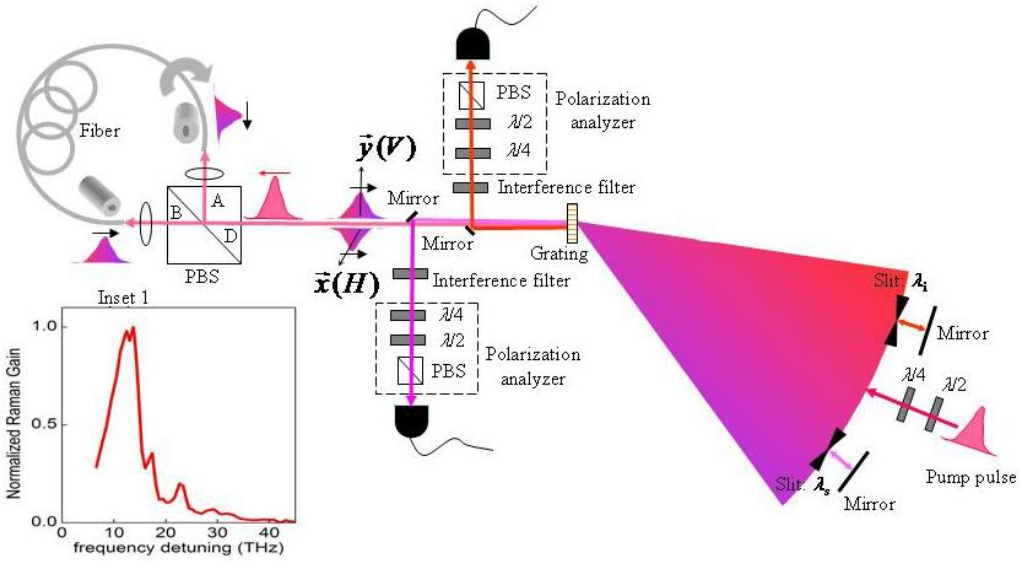

FIG. 4 Schematic of the experimental setup. PBS: polarizing beam splitter, λ/2: half wave plate, λ/4: quarter wave plate, M: mirror. Inset 1 is the measured Raman spectral profile of the fiber in use.

With a two-pass grating configuration,[14] the Bell state $\Phi^+ = H_s H_i + V_s V_i$ (ω is dropped for simplicity), at a particular frequency with a collection bandwidth of $\Delta\omega$ = 0.5 THz (0.9 nm), is selected simply by moving the slits shown in Fig. 4 to a pair of positions that are calibrated to select conjugate signal and idler wavelengths that are connected by energy conservation. The use of the two-pass grating configuration not only maintains the selected photons in single spatial modes, but also provides better spectral rejection of other wavelengths. The other three Bell states are created by appropriate orientations of the quarter (λ/4) and half (λ /2) wave plates in the pump, and/or in the signal (or the idler) beam paths. The Bell states produced are measured using a polarization analyzer and single-photon detector (Si avalanche photo-diode) in the signal and idler beam paths. The detector signals are sent to a logic circuit to count the coincidences and accidental coincidences. Each polarization analyzer consists of, in order, a λ/4-wave plate, a λ/2-wave plate, and a PBS.

The Bell state $\Phi^+ = H_s H_i + V_s V_i$ created at the PBS passes through many optical elements before entering the polarization analyzer. In practice, the transmission efficiency of an optical element is less than unity and can vary with wavelength and polarization. Assuming more loss of V-polarized photons than H-polarized photons during propagation, the entangled quantum state becomes $\chi = H_s H_i + c V_s V_i$ with $c <$ 1, when it enters the analyzer. To eliminate this polarization imbalance, one can actively introduce more loss to H-polarized photons to equalize the amplitudes for the H_sH_i and V_sV_i terms. Instead of using this method, we rotate the polarization of the pump pulse to increase the relative probability of producing a V-polarized bi-photon state. The use of unequal pump power for the two pump pulses also produces different self-phase modulation (of the pump pulse) and cross-phase modulation (induced by the pump pulse to the created photons) in the two nonlinear processes in the PMMF, yielding a relative phase difference 2φ between the two created bi-photon states H_sH_i and V_sV_i. Thus the quantum state at the PBS is $\chi = H_s H_i + (1/c)e^{i2\varphi} V_s V_i$. After passing through various optical elements to enter the polarization analyzers, the state becomes $\chi = H_s H_i + e^{i2\varphi} V_s V_i$. Here the system-induced relative phase difference between the two bi-photon states H_sH_i and V_sV_i (for example, the residual material birefringence of the optical elements can cause different phase retardations to the H- and V- polarized photons) is stable and is absorbed into 2φ, and the overall phase term is dropped for simplicity. It is known that rotations of the λ/2-wave plate and the λ/4-wave plate in the pump beam path can make $2\varphi = 0$ or π to make the Bell states

$\Phi^{\pm} = H_s H_i \pm V_s V_i$.[15] In addition, rotating a $\lambda/2$-wave plate in the signal beam path by 45° allows the other two Bell states $\Psi^{\pm} = V_s H_i \pm H_s V_i$ to be prepared.

4. Two-photon quantum interference visibility and Bell test

In a previous work,[16] we examined the gain spectra of the Raman scattering and SFWM in this PMMF. We measured a 10 THz (≈24 nm) 3dB bandwidth for the production of bi-photon states with high spectral brightness and small background. Based on that measurement, for the current experiment we set the slits in the signal and idler paths to select λ_s = 689 nm and λ_i = 800 nm with $\Delta\lambda$ = 0.9 nm (0.5 THz), all within the 10 THz band. We measured the quantum-interference fringe visibilities of the Bell state $\Phi^{+} = H_s H_i + V_s V_i$ at four different angle settings θ_s, for the polarization analyzer in the signal arm: θ_s = 0°, 45°, 90°, -45°. The visibility is defined as $V = (C_{max} - C_{min})/(C_{max} + C_{min})$, where C_{max} and C_{min} are the maximum and minimum coincidence count rates, respectively. The coincidence rates oscillate sinusoidally with the angle of the polarization analyzer (θ_i) in the idler arm as shown in Fig. 5. With a total average pump power of 300 μW, we measured a maximum coincidence rate of 7 kHz at a brightness of 26 kHz $nm^{-1}mW^{-1}$. The visibilities calculated based on the fit parameters are listed in Table 1. Without subtracting accidental coincidences, the visibilities are > 91% for all four values of θ_s. After subtracting the accidental coincidence, the visibilities are > 97%. While the two-photon detection *rate* of the best down-conversion-based sources[7-9] is currently larger than what we have demonstrated with a fiber-based source, the two-photon *brightness* per unit pump power demonstrated for our fiber-based source surpasses the best value demonstrated for any down-conversion source.

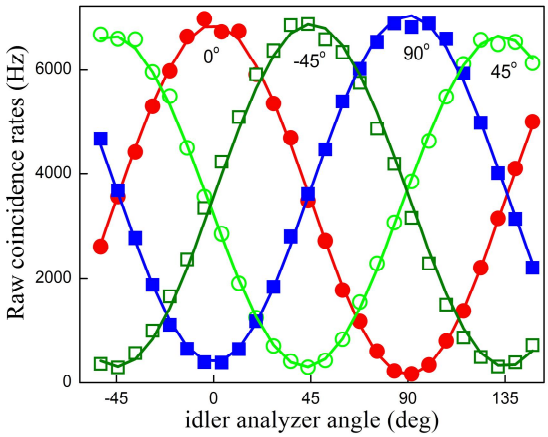

Fig. 5 Raw coincidence count rates as a function θ_i for four different values of θ_s (0°, 45°, 90°, -45°) along with fits to $\sin^2(\theta_i)$ (lines). A 10 s integration time was used for each point. λ_s = 689 nm and λ_i = 800 nm.

Table 1. Quantum-interference fringe visibility.

θ_s (deg)	Visibility (%) (raw)	Visibility (%) (accidentals subtracted)
0	95.8 ± 1.1	100 ± 1.2
45	91.3 ± 1.0	97.6 ± 1.1
90	91.6 ± 1.1	97.5 ± 1.2
-45	91.3 ± 0.5	97.1 ± 0.6

We measured the *S* parameter, a test of nonclassicality defined by the Clauser-Horne-Shimony-Holt form of Bell's inequality.[17] The analyzer settings in the signal arm were θ_s = 0°, 90°, -45°, 45° and in the idler

arm were θ_i = -22.5°, 67.5°, 22.5°, 112.5°, totaling 16 coincidence measurements. Each measurement setting took 10 s to complete with the resulting S values listed in Table 2. In less than 3 minutes for each Bell state, we demonstrated a violation of the classical limit of S = 2 by more than 20 standard deviations. S was calculated using raw coincidence data with no subtraction of accidentals.

Table 2. Measured value of S for all four Bell states.

Bell state	S	Violation (σ)
$H_sH_i + V_sV_i$	2.622 ± 0.016	37
$V_sH_i + H_sV_i$	2.567 ± 0.016	34
$V_sH_i - H_sV_i$	2.321 ± 0.014	22
$V_sV_i + H_sH_i$	2.408 ± 0.015	27

Our two-pass grating configuration allows us select Bell states at different wavelengths by simply translating slits in the signal and idler paths to different predetermined positions. By moving the slits from previous settings to select λ_s = 693 nm and λ_i = 795 nm, without any additional optical alignment, we immediately obtain the Bell state $\Phi^+ = H_sH_i + V_sV_i$ at the new wavelengths. The two-photon coincidence rate remains at the 7 kHz level. The quantum interference fringe visibilities remain > 97% (with accidentals subtracted), as shown in Fig. 6. The measured S parameter of 2.490 ± 0.015, violates the classical limit by 32 standard deviations.

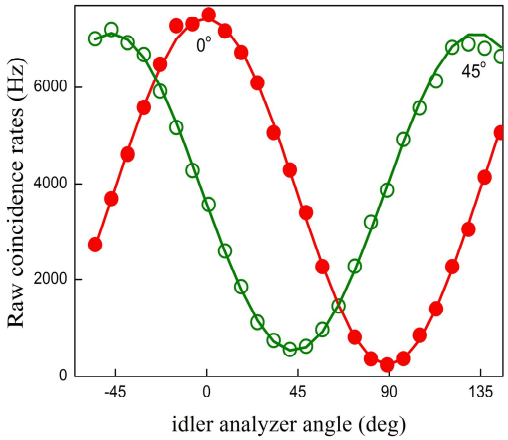

Fig. 6 Raw coincidence count rates (dots) as a function of θ_i for two different values θ_s (0°, 45°) along with fits to $\sin^2(\theta_i)$ (lines). A 10 s integration time was used for each point. λ_s = 693 nm and λ_i = 795 nm.

5. Conclusions

We have proposed and demonstrated a robust high spectral brightness, broad wavelength coverage, single-spatial mode source of polarization-entangled photon pairs with high two-photon visibility and phase-stability. This source has two-photon flux comparable to the best yield of down-conversion sources while having the ability and flexibility to simultaneously output entangled photon pairs at multiple wavelengths at the same high mode brightness to allow the operation of wavelength-division-multiplexing.

In addition, the gain and dispersion of microstructure fiber can be controlled through design of the fiber's physical structure, such as the core size and air-hole size, as well as by choosing materials with higher nonlinearity. This should enable even higher two-photon production rates with lower background, as well as allowing pair production at wavelengths ranging from ultraviolet to infrared, meeting the requirements of more quantum-information applications. Although in an early development stage, this bright, phase-stable, wavelength tunable, single-mode fiber-based source of polarization-entangled photon pairs is already comparable to the best performing down-conversion-based sources. With its wavelength tunability

and inherent mechanical stability, this source is a promising candidate for use in practical, real-world, quantum-information science applications.

Understandably, this new technique is still at its infancy, merely a few years after it was first proposed. However, it's already showing promise. With more R&D effort, particularly from the engineering aspect, it is conceivable that one day a cheap, robust, plug-and-play polarization-entangled two-photon source will be available, for real world cryptography systems.

This work has been supported in part by the Disruptive Technology Office (DTO) entangled photon source program, and the Multidisciplinary University Research Initiative Center for Photonic Quantum Information Systems (Army Research Office/DTO program DAAD19-03-1-0199). MDE acknowledges support from the National Research Council (NRC).

REFERENCES

1. C. Cinelli, M. Barbieri, R. Perris, P. Mataloni, and F. De Martini, "All-Versus-Nothing Nonlocality Test of Quantum Mechanics by Two-Photon Hyperentanglement," *Phys. Rev. Lett.* 95, 240405 (2005).
2. H. Takesue, E. Diamanti, T. Honjo, C. Langrock, M. M. Fejer, K. Inoue, Y. Yamamoto, "Differential phase shift quantum key distribution experiment over 105 km fibre," *New Journal of Physics* 7, 232 (2005).
3. C. Bennett, G. Brassard, C. Crepeau, R. Jozsa, A. Peres, and W. K. Wootters, "Teleporting an unknown quantum state via dual classical and Einstein-Podolsky-Rosen channels," *Phys. Rev. Lett.* 70, 1895 (1993).
4. D. Boumeester, J. W. Pan, K. Mattle, M. Eibl, H. Weinfurter, and A. Zeilinger, "Experimental quantum teleportation,", *Nature* (London) 390, 575 (1997).
5. A. K. Ekert, "Quantum cryptography based on Bell's theorem," *Phys. Rev. Lett.* 67, 661 (1991).
6. D. C. Burnham, and D. L. Weinberg, "Observation of Simultaneity in Parametric Production of Optical Photon Pairs," *Phys. Rev. Lett*. 25, 84-87 (1970).
7. P. G. Kwiat, E. Waks, A. G. White, I. Appelbaum, and P. H. Eberhard, "Ultrabright source of polarization-entangled photons," *Phys. Rev*. A 60, R773-776 (1999).
8. C. Kurtsiefer, M. Oberparleiter, and H. Weinfurter, "High-efficiency entangled photon pair collection in type-II parametric fluorescence," *Phys. Rev.* A 64, 023802 1-4 (2001).
9. J. Altepeter, E. Jeffrey, P. G. Kwiat, "Phase-compensated ultra-bright source of entangled photons,"*Opt. Express* 13, 8951-8959 (2005).
10. G. P. Agrawal, *Nonlinear Fiber Optics*, 2nd edition (Academic, New York, 1995).
11. J. C. Knight, T. A. Birks, P. St. J. Russell, D. M. Atkin, "Endlessly single-mode photonic crystal fiber,"*Opt. Lett.* 21, 1547 (1996).
12. X. Li, P. Voss, J. E. Sharping, J. Chen, and P. Kumar, "Optical-Fiber Source of Polarization-Entangled Photons in the 1550 nm Telecom Band ,"*Phys. Rev. Lett*. 94, 053601 (2005).
13. H. Takesue and K. Inoue, "Generation of polarization-entangled photon pairs and violation of Bell's inequality using spontaneous four-wave mixing in a fiber loop ,"*Phys. Rev*. A 72, 041804(R) (2005).
14. J. Fan, A. Migdall, and L. J. Wang, "Efficient generation of correlated photon pairs in a microstructure fiber**,"** *Opt. Lett.* 30, 3368 (2005).
15. T. Kim, M. Fiorentino, and N. C. Wong, "Phase-stable source of polarization-entangled photons using a polarization Sagnac interferometer," *Phys. Rev*. A 73, 012316 (2006).
16. J. Fan and A. Migdall, "A broadband high spectral brightness fiber-based two-photons source," *Opt. Express* 15, 2915-2920 (2007).
17. J. F. Clauser, M. A. Horne, A. Shimony, and R. A. Holt, "Proposed Experiment to Test Local Hidden-Variable Theories," *Phys. Rev. Lett*. 23, 880 (1970).